

Noniterative equilibria reconstruction without up-down symmetry

P. Rodrigues and J. P. S. Bizarro

*Associação Euratom—IST, Instituto de Plasmas e Fusão Nuclear,
Instituto Superior Técnico, 1049–001 Lisboa, Portugal.*

In usual iterative equilibria reconstructions [1], the Grad-Shafranov (GS) equation has its nonlinear source term set to a predefined model depending on a few parameters which are then iteratively chosen in order to fit some measured internal profiles (e.g., plasma pressure, field pitch, etc.) as well as boundary conditions and some other global data. The iterative procedure arises because such input profiles are actually measured in laboratory rather than flux coordinates, which are themselves unknowns of the reconstruction problem [2, 3]. In contrast, non-iterative reconstruction schemes are designed with the intention to keep the measured profiles fixed along a given chord throughout the reconstruction process, allowing the GS equation to be solved, directly in laboratory coordinates, in one single step [4]. This approach becomes handy whenever iterative computations run into convergence problems, grow into a time-consuming burden (real-time equilibria reconstruction), or if solutions without nested flux surfaces are needed (toroidal current reversal).

A noniterative algorithm has been developed [4] subject to the condition that the poloidal magnetic-field flux must display up-down symmetry [i.e., $\psi(r, \theta) = \psi(r, -\theta)$], being thus represented by the even trigonometric series

$$\psi(r, \theta) = \psi_0(r) + \sum_{n=1}^{+\infty} \sum_{k=0}^n \frac{\varepsilon^n}{n!} \hat{\psi}_{nk}(r) \cos k\theta, \quad (1)$$

where r is the radial distance to the magnetic axis normalized to the minor radius a , θ is a poloidal angle measured clockwise from the midplane at the high-field side, and $\varepsilon = a/R_0$ is the inverse aspect ratio, with R_0 the major radius. It has been shown that inserting the series (1) into the GS equation

$$-R^2 \nabla \cdot (R^{-2} \nabla \psi) = R^2 \dot{p}(\psi, \varepsilon) + \dot{Y}(\psi, \varepsilon), \quad (2)$$

for which $R = 1 - \varepsilon r \cos \theta$, p and Y are, respectively, the normalized plasma pressure and the squared poloidal current, and the dot stands for a flux derivative $d/d\psi$, yields the zeroth-order condition $r^{-1}(r\psi_0')' = \dot{p}_0 + \dot{Y}_0$ and the sequence of linear equations

$$r^2 \hat{\psi}_{nk}''(r) + r \hat{\psi}_{nk}'(r) + [s(r) - k^2] \hat{\psi}_{nk}(r) = \hat{b}_{nk}(r), \quad (3)$$

providing each $\hat{\psi}_{nk}$ computed from the source $\hat{b}_{nk} = [(1 + \delta_{0k})\pi]^{-1} \int_{-\pi}^{\pi} b_n(r, \theta) \cos k\theta d\theta$, where δ_{nk} is the Kronecker delta and $b_n(r, \theta)$ involves lower-order terms only [4].

To handle configurations where the up-down symmetry is not acceptable (single nulls, for instance), odd harmonics must be added to the series (1), which becomes

$$\psi(r, \theta) = \psi_0(r) + \sum_{n=1}^{+\infty} \frac{\varepsilon^n}{n!} \sum_{k=0}^n \hat{\psi}_{nk}(r) \cos k\theta + \check{\psi}_{nk}(r) \sin k\theta. \quad (4)$$

After plugging the latter into the GS equation (2) and collecting for the same powers of ε , one gets another set of equations,

$$r^2 \check{\psi}_{nk}''(r) + r \check{\psi}_{nk}'(r) + [s(r) - k^2] \check{\psi}_{nk}(r) = \check{b}_{nk}(r), \quad (5)$$

providing each odd component $\check{\psi}_{nk}$ in terms of the source $\check{b}_{nk}(r) = \pi^{-1} \int_{-\pi}^{\pi} b_n(r, \theta) \sin k\theta d\theta$ and which must be considered in addition to the one in (1). When writing the series (4), it is implicit that each n -th order contribution has its spectral content limited to n harmonics, both even and odd. While the limit regarding the former has been firmly established [4], the limit concerning the latter can be easily arrived at by following the same reasoning, with the aid of only a couple of additional trigonometric identities.

At its core, the noniterative algorithm takes advantage of the explicit dependence on ε in the right-hand side of (2), which is unknown at the start of the reconstruction, tailoring it in such a way that any computed n -th order correction will not change any two independent input profiles along two chords of constant θ , where only their zeroth order terms survive. The reconstruction procedure is simplified if the input profiles are chosen to be the plasma pressure $P(r)$ and the vertical field $B_{(z)}(r)$, measured along the plasma midplane. These enable one to set the experimental zeroth order terms $p_0(r) \propto P(r)$ and $\psi_0(r) \propto \int_0^r RB_{(z)}(u)du$, and after require them to remain unchanged throughout $\theta = \pi$. The choice of the suitable explicit dependence on ε in (2) allowing these requirements to be fulfilled is described elsewhere [4] and does not change even if (4) replaces the series (1).

The noniterative algorithm described above is next employed to reconstruct the magnetic equilibrium of a DIII-D discharge (#111239) where the profiles $B_{(z)}(r)$ and $P(r)$ are measured by motional Stark effect (MSE) polarimetry very close to the plasma midplane [5]. Setting $R_0 = 1.78\text{m}$ (where $B_{(z)}$ crosses zero) and $a = 0.52\text{m}$ (due to vessel geometry constraints), the low-field side data points are first fitted by suitable 1D rational-function models, yielding two smooth functions, $P(r)$ and $B_{(z)}(r)$, defined for $0 \leq r \leq 1$ and which are afterwards fed to the reconstruction algorithm. Perturbations up to the third order in ε are considered, demanding a total of six boundary conditions to be supplied when solving the sets (3) and (5), respectively, $\hat{\psi}_{22}(1)$, $\hat{\psi}_{32}(1)$, and $\hat{\psi}_{33}(1)$ for the even part, and $\check{\psi}_{22}(1)$, $\check{\psi}_{32}(1)$, and $\check{\psi}_{33}(1)$ for the odd one. Without any information about the last closed flux surface, these are chosen in order to make the inner separatrix hit the lower divertor and the resulting equilibrium is depicted in Fig. 1.

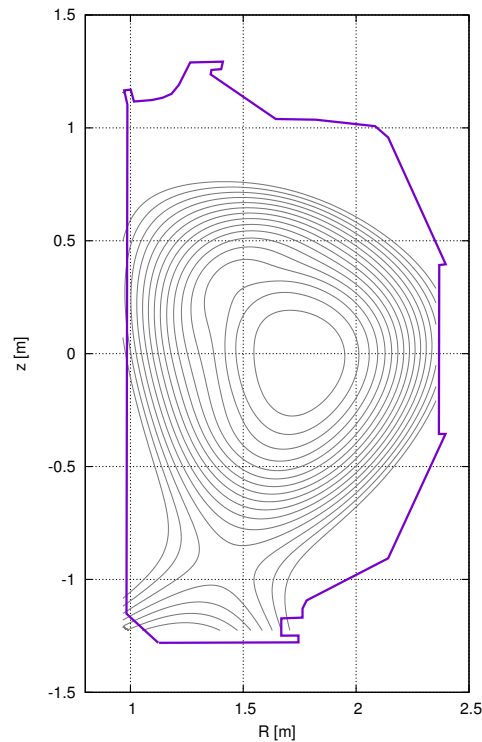


Figure 1: Surfaces of constant poloidal-field flux.

The experimental data is displayed in Fig. 2, together with the reconstruction results. Not surprisingly, the computed profiles closely match all low-field side data points, precisely along the chord where the algorithm is designed to keep them fixed while new perturbations are being added. Conversely, the high-field side data points do not contribute to the algorithm, but their proximity to the predicted profile signals an overall consistent reconstruction. While this is particularly true for the MSE data, the discrepancies in the pressure may be due to inaccuracies in the way their estimates are produced [5].

In conclusion, a noniterative reconstruction algorithm has been extended to cope with magnetic configurations without up-down symmetry and its ability to handle real experimental data has been shown.

Acknowledgments

This work has been carried out within the framework of the Contract of Association between the European Atomic Energy Community and the Instituto Superior Técnico (IST), and has also received financial support from the Fundação para a Ciência e a Tecnologia (FCT). The content of this paper is the sole responsibility of the authors and it does not necessarily represent the views of the European Commission, of FCT, of IST, or of their services.

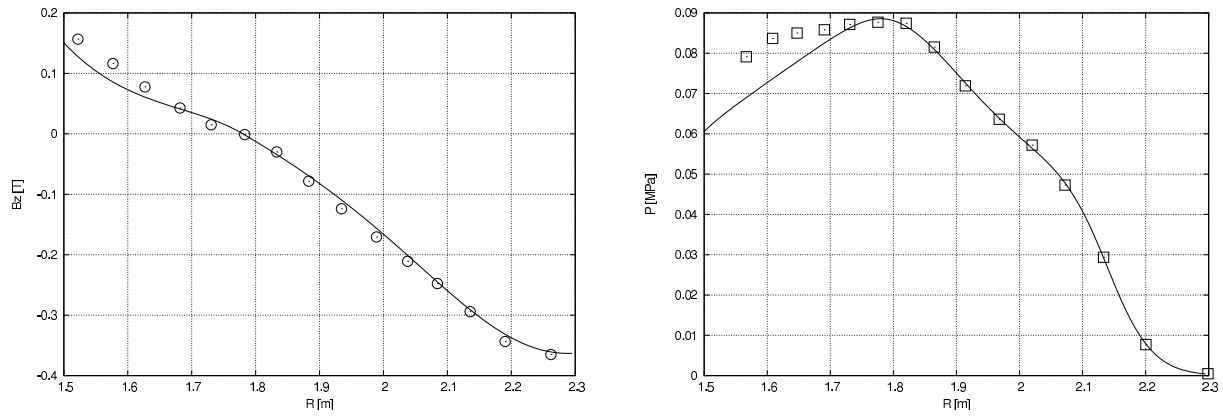


Figure 2: Measured vertical field B_z (open circles) and plasma pressure P (open squares) together with the corresponding reconstructed profiles (solid line).

References

- [1] L. L. Lao, H. St. John, R. D. Stambaugh, A. G. Kellman, and W. Pfeiffer, Nucl. Fusion **25**, 1611 (1985).
- [2] J. M. Greene, J. L. Johnson, and K. E. Weimer, Phys. Fluids **14**, 671 (1971).
- [3] L. L. Lao, S. P. Hirshman, and R. M. Wieland, Phys. Fluids **24**, 1431 (1981).
- [4] P. Rodrigues and J. P. S. Bizarro, Phys. Plasmas **11**, 186 (2004).
- [5] C. C. Petty, P. A. Politzer, and Y. R. Lin-Liu, Plasma Phys. Control. Fusion **47**, 1077 (2005).